reactions

Article

Obtaining Biodiesel from Soybean Vegetable Oil Using a Hydrodynamic Cavitation Reactor

Luz Clara Andia-Marron [1,*], Jessica Abad-Salcca [1], Juan Taumaturgo Medina-Collana [1,*], Edgar Williams Villanueva-Martinez [1], Jorge Amador López-Herrera [1], Richard Brandon Guevara-Salcedo [1], Leonard Ordoñez-Santa Maria [1], Rodolfo Paz-Salazar [1], Fredy Andrés Taipe-Castro [1], Jorge Alberto Montaño-Pisfil [2] and Segundo Alberto Vásquez-Llanos [3]

[1] Centro de Investigación de Ingeniería de Procesos de Tratamiento de Aguas, Facultad de Ingeniería Química, Universidad Nacional del Callao, Bellavista 07011, Peru; jabads@unac.edu.pe (J.A.-S.); ewvillanuevam@unacvirtual.edu.pe (E.W.V.-M.); jalopezh@unac.edu.pe (J.A.L.-H.); rbguevaras@unac.edu.pe (R.B.G.-S.); lordonezsm@unac.edu.pe (L.O.-S.M.); rpazs@unac.edu.pe (R.P.-S.); fataipec@unac.edu.pe (F.A.T.-C.)
[2] Facultad de Ingeniería Eléctrica y Electrónica, Universidad Nacional del Callao, Bellavista 07011, Peru; jamontanop@unac.edu.pe
[3] Grupo de Investigación CIMAYDS, Facultad de Ingeniería Química e Industrias Alimentarias, Universidad Nacional Pedro Ruiz Gallo, Lambayeque 14013, Peru; savasquez@unprg.edu.pe
* Correspondence: lcandiam@unac.edu.pe (L.C.A.-M.); jtmedinac@unac.edu.pe (J.T.M.-C.)

Abstract

Hydrodynamic cavitation (HC) is an efficient technique for biodiesel production. The main contribution of this study is the development of a modular reactor with a universal stainless steel joint, whose design facilitates the installation, replacement, and maintenance of the orifice plate by eliminating flanges and bolts during assembly. Using this reactor, the study evaluated the synergistic interaction between feed pressure and methanol:oil molar ratio in the transesterification of soybean oil, employing a 3^2 factorial design. The orifice plate was 3 mm thick and had 19 holes with a diameter of 1.0 mm, installed downstream of the pump. The process was carried out for 45 min, using NaOH at 1 wt% relative to the oil and at 60 ± 5 °C. Feed pressures of 1.72, 2.41, and 3.10 bar and methanol:oil molar ratios of 6:1, 8:1, and 10:1 were evaluated, reaching a maximum yield of 92.98% at 3.10 bar and 8:1. Analysis of variance (ANOVA) confirmed a significant interaction ($p < 0.0001$) and allowed a second-order polynomial model to be fitted ($R^2 = 0.9981$). In contrast, conventional mechanical agitation required 90 min to achieve 95% yield. The biodiesel produced met most American Society for Testing and Materials (ASTM) D6751 requirements, confirming the potential of HC as a viable alternative for intensifying biodiesel production.

Keywords: biodiesel; hydrodynamic cavitation; transesterification; soybean oil; orifice plate reactor; process intensification; response surface methodology

Academic Editors: Diogo M.F. Santos, Catarina Nobre, Paulo Brito and Margarida Gonçalves

Received: 2 January 2026
Revised: 2 March 2026
Accepted: 3 March 2026
Published: 6 March 2026

1. Introduction

The energy crisis and climate change are critical challenges of the 21st century. The transport sector, responsible for 24% of global CO_2 emissions, requires solutions aligned with Sustainable Development Goal 7 [1]. In 2024, fossil fuels accounted for >80% of global energy consumption (648 EJ), while renewables reached only 15% [2], with global greenhouse gas (GHG) emissions of 57.1 Gt CO_2-eq, of which 37.6 Gt corresponded to fuel combustion [3]. Without mitigation policies, the projected temperature increase could reach

3.1 °C by the end of the century [4]. In this context, biodiesel has emerged as a sustainable alternative, with an estimated production of 64.1 billion liters in 2026, highlighting the growing role of biofuels in the transition toward low-carbon energy systems [5]. Biodiesel reduces GHG emissions by more than 50% compared to gasoline [6], and by 79–86% in life cycle analysis when produced from used oils, although its blending with diesel is restricted to 20% without engine modifications [7]. It contains less carbon, higher oxygen content, and no sulfur or aromatics, generates lower SO_x and NO_x emissions [8], has a high cetane number and stability in blends with fossil diesel [9,10], and is essential for achieving net zero emissions [11,12].

Biodiesel is synthesized by transesterification of triglycerides with methanol, producing fatty acid methyl esters (FAME) and glycerol [13], as shown in Figure 1. Raw materials include edible and non-edible oils, animal fats, and recycled oils [14], classified according to their origin into four generations: first (food crops), second (non-edible or used oils), third (microalgae) [15], and fourth (genetically modified microorganisms) [16]. Although waste oils reduce production costs, their high water and free fatty acid (FFA) content can affect performance [17,18], which is why soybean oil is widely used due to its low moisture and FFA content [19].

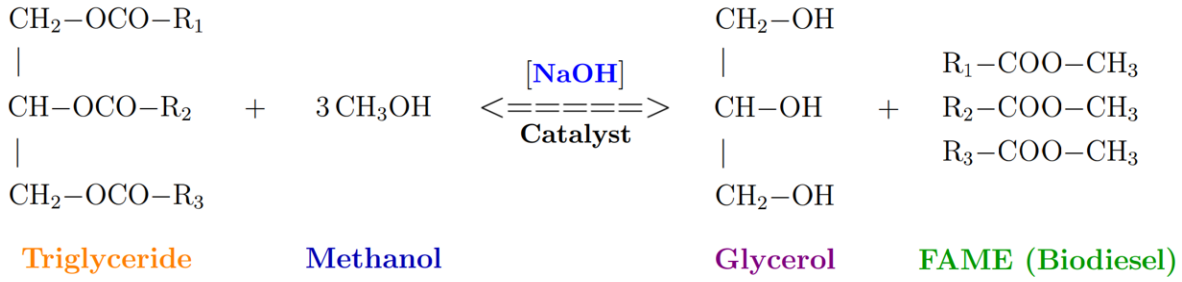

Figure 1. Transesterification of triglycerides with methanol to produce FAME and glycerol.

Industrially, transesterification is mainly carried out with homogeneous alkaline catalysts, such as NaOH or KOH, and operated at 60–65 °C for 30–60 min, achieving yields of over 90% [20]. These catalysts have significantly faster kinetics than acids such as HCl or H_2SO_4 [21], which require higher temperatures, longer times, and cause corrosion problems [22]. However, alkaline catalysts react with free fatty acids (FFA) to form soaps, which reduces yield and hinders the separation and purification of biodiesel [23]. This phenomenon intensifies when the acid value exceeds approximately 1 mg KOH/g [24,25] or in the presence of water, decreasing FAME production [26]. As alternatives, heterogeneous catalysts such as CaO and K_2CO_3, among others [27,28], have been studied, which facilitate separation and reuse, allowing in some cases simultaneous transesterification and esterification [29]. Lipases [8] and technologies such as supercritical alcohol processing [30], microemulsions [31], and pyrolysis [11] have also been evaluated.

HC has emerged as an innovative technology capable of overcoming several of these limitations. Cavitation can be classified as hydrodynamic, acoustic [32], optical, and particle [33]. In HC, pressure fluctuations induced by local velocity variations when passing through geometric constrictions generate the formation and collapse of bubbles [34]. This collapse releases localized energy, reaching temperatures close to 5000 K and pressures of around 1000 bar [35], as well as generating highly reactive radicals such as •OH [36], which have been widely studied in water treatment [37]. In biodiesel production, HC intensifies the interfacial mixing between methanol and oil, overcoming the natural immiscibility of the system, accelerating the reaction rate, and increasing triglyceride conversion [13]. HC systems consist of a storage tank, high-

pressure pump, control valves, and reactor [38]. Reactors are classified as rotational, including rotor-stator designs [39] and shock wave power reactors (SPR) [40], and non-rotational, comprising Venturi devices and orifice plates, widely used for their simple and efficient design [36]. During the cavitation process, the contact area between reactants increases exponentially, overcoming the mass transfer barriers that limit mechanical agitation. In addition, HC eliminates the formation of soaps that complicate purification in conventional processes [23,24] and reduces energy consumption [25], addressing one of the main production cost factors that limit the economic competitiveness of biodiesel compared to fossil fuels [41].

The superiority of HC over conventional methods has been consistently demonstrated in multiple studies. With soybean oil, HC reduced the reaction time from 120 to 17 min (an 86% reduction), achieving >96.5% FAME content with a methanol:oil molar ratio of 12:1 and 0.5 wt% NaOH [42]. With waste soybean oil, 100-hole plates with 0.3 mm holes achieved 99% yield in 5 min with a molar ratio of 6.8:1 and 1 wt% NaOH [43], representing a 92–96% reduction in time compared to conventional methods.

Other studies include *Hippophae rhamnoides* oil, achieving FAME content greater than 96.5% using 1 mm plates with 21 holes at 3 bar and 60 °C [44]. For *Cannabis sativa* L. oil, 97.5% conversion was achieved in 20 min using a 7-hole plate with 3 mm holes at 3 bar, 1 wt% KOH, and 60 °C, reducing the time by 78% compared to mechanical agitation [45]. Regarding rubber seed oil, 97.1% conversion was obtained in 20 min with a 50 L reactor, 21-hole plate with 1 mm holes, 6:1 methanol:oil ratio, 1 wt% KOH, 3 bar, and 55 °C, reducing the time fivefold compared to mechanical agitation [46]; and castor oil optimized by response surface methodology, achieving 92.27% conversion with a molar ratio of 9.82:1, 60.3 °C, 1.06 wt% KOH, and 2 bar [34].

Despite reported advances in intensifying the process through HC, there remains a knowledge gap in the specific optimization of operating parameters for soybean oil. In particular, the synergistic effect between feed pressure and the methanol:oil molar ratio has not been fully established, limiting the rigorous definition of optimal conditions for industrial implementation. Furthermore, conventional designs of HC reactors, based on flange and bolt systems, have practical limitations associated with maintenance, cleaning, and replacement of orifice plates, increasing downtime and operating costs.

The primary novelty of this study lies in the development of a modular hydrodynamic cavitation reactor incorporating a universal stainless steel joint that eliminates the need for flanges and bolts. This design enables rapid assembly and disassembly of the orifice plate, significantly improving accessibility, operational efficiency, and maintenance conditions while reducing system downtime. Additionally, the study systematically evaluates the interaction between feed pressure and the methanol:oil molar ratio in soybean oil, contributing to the rigorous definition of optimal operating conditions with potential application in industrial scale-up.

This configuration suggests an improvement in the operational feasibility of hydrodynamic cavitation reactors, with possible implications for their implementation at larger scale in sustainable biodiesel production.

2. Materials and Methods

2.1. Raw Materials and Reagents

Commercial soybean oil (*Glycine max*) of the brand "Venecia" was used as raw material, purchased at the Tantamayo market, San Martín de Porres district, Lima, Peru. Although soybean oil is classified as a first-generation raw material for biodiesel, it was selected due to its well-characterized composition, high availability, and experimental reproducibility,

which allows for a controlled evaluation of the HC process. The physicochemical properties and fatty acid composition of the oil used are presented in Table 1.

Table 1. Properties of the commercial soybean oil used in this study.

Property	**This Study**
Acid value (mg KOH/g)	0.04
Moisture content (wt%)	0.03
Density at 15 °C (g/mL)	0.920
Fatty acids (%)	
Palmitic (C16:0)	11.2
Stearic (C18:0)	4.1
Oleic (C18:1)	23.5
Linoleic (C18:2)	53.8
Linolenic (C18:3)	7.4

The oil had a low acid value (0.04 mg KOH/g) and low moisture content (0.03 wt%), confirming its suitability for alkaline transesterification with NaOH, minimizing the risk of saponification derived from free fatty acids or the presence of water. The fatty acid composition, predominantly unsaturated, corresponds to that expected for refined commercial soybean oil.

The chemical reagents used included American Chemical Society (ACS) grade methanol (≥99.8%) and ACS grade sodium hydroxide (NaOH) (≥99%) as the main reagents for transesterification; hydrochloric acid (37%), ACS ethyl alcohol (≥99.5%), ACS acetone (≥99%), ACS potassium biphthalate (≥99%), and ACS bromophenol blue (≥99%) as auxiliary reagents; and distilled water as a solvent. The high purity of all reagents ensures experimental reproducibility and minimizes the formation of unwanted by-products. All reagents were purchased from CIMATEC S.A.C., Lima, Perú.

2.2. Experimental Setup

2.2.1. Hydrodynamic Cavitation System

The experimental HC system was designed to evaluate biodiesel production, as shown in Figure 2. The setup consisted of a closed recirculation circuit, which integrated a jacketed storage tank, a centrifugal pump, an orifice plate reactor, and a set of measurement and control instruments.

The storage tank was a stainless steel cylinder with an external jacket, with a total capacity of 6 L, using a working volume of 3 L per test. The jacket allowed the reaction temperature to be maintained at 60 ± 5 °C by circulating temperature-controlled water. The reaction mixture was continuously recirculated through the reactor, where most of the cavitation phenomenon was concentrated.

The centrifugal pump, with a maximum nominal pressure of 11.38 bar, was installed at the base of the reactor to draw in and recirculate the fluid. The evaluated pressure range (1.72–3.10 bar) falls within the operating conditions commonly reported for HC devices applied to biodiesel production, coinciding with previous experimental studies and supporting the practical relevance and applicability of the selected range in continuous flow systems [44,47].

The system instrumentation included:

- Two pressure gauges: P1 upstream and P2 downstream of the orifice plate, to measure the pressure drop across the cavitator.

- Three flow control valves: V1 on the main line to regulate flow through the cavitator; V2 on the bypass line to adjust recirculation and pressure; and V3 for controlled emptying of the glycerol phase during crude biodiesel separation.
- An in-line flowmeter to monitor system flow and ensure stable conditions during testing.

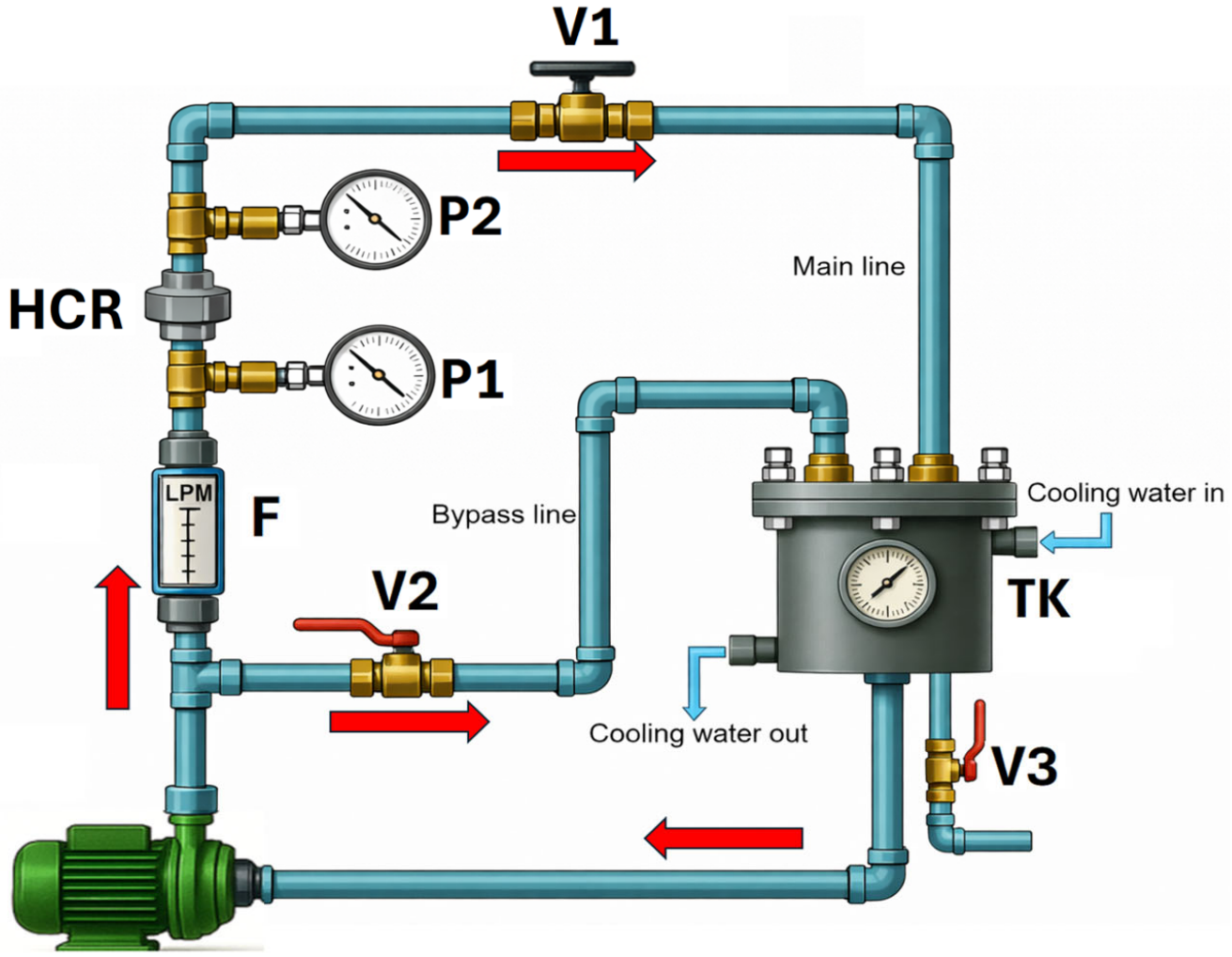

Figure 2. Schematic diagram of the experimental hydrodynamic cavitation system. It includes a jacketed storage tank (TK), centrifugal pump (P), hydrodynamic cavitation reactor (HCR), pressure gauges (P1 and P2), flowmeter (F, in liters per minute, LPM), and flow control valves (V1, V2, V3). The arrows indicate the direction of flow during operation.

2.2.2. Hydrodynamic Cavitation Reactor and Orifice Plate

The HC reactor consisted of an orifice plate housed in a stainless steel universal joint, designed to allow the plate to be assembled, disassembled, and replaced without modifying the rest of the system, as shown in Figure 3. The assembly consisted of a threaded bushing, which supports the other components of the universal joint; an O-ring, placed between the unthreaded bushing and the orifice plate; the orifice plate, circular and flattened, which constitutes the active zone of the reactor; a rubber gasket in the shape of a flattened circular crown; an unthreaded bushing, which also acts as a support; and a nut with an internal thread, which connects both bushings and houses the orifice plate, so that its internal diameter matches that of the plate. This construction ensures secure assembly and allows for efficient maintenance and cleaning operations without affecting the integrity of the experimental system, while also ensuring low-cost equipment in both implementation and operation.

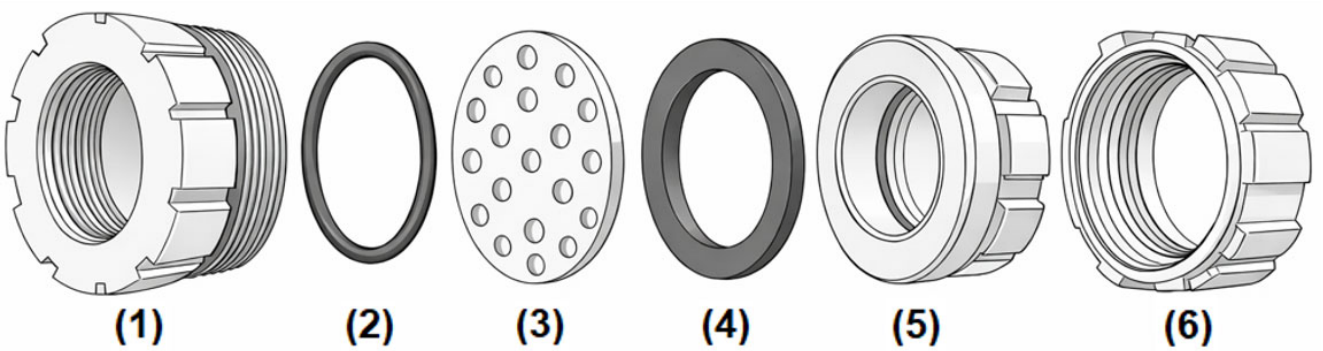

Figure 3. Exploded view of the cavitator device with universal joint. From left to right: (**1**) threaded bushing, (**2**) O-ring, (**3**) orifice plate, (**4**) gasket, (**5**) unthreaded bushing, and (**6**) nut with internal thread.

A 25 mm diameter plate with 19 holes measuring 1.0 mm in diameter and 3 mm in thickness was selected and positioned vertically downstream of the pump. The vertical orientation allows stable and efficient cavitation to be generated, optimizing bubble formation and collapse, which increases mass transfer during transesterification, as reported in previous studies [48,49].

The hole layout pattern was concentric: 1 central hole, 6 in an inner ring (radius 5 mm), and 12 in an outer ring (radius 10 mm), with an average center-to-center separation of 5 mm, as shown in Figure 4. The choice of 19 holes optimizes flow distribution, ensuring homogeneous cavitation.

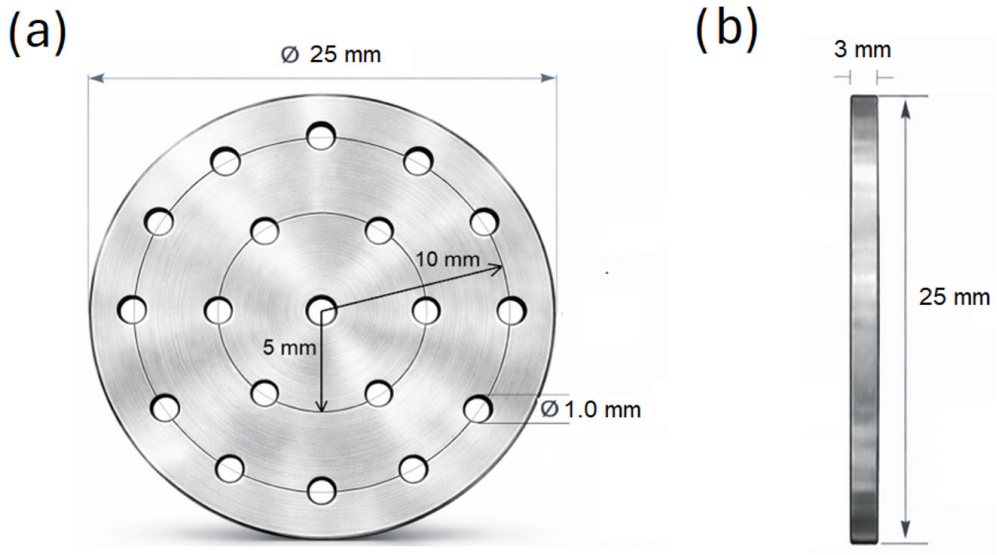

Figure 4. Geometric configuration of the orifice plate. (**a**) Front view showing concentric pattern; (**b**) side view indicating thickness (3 mm) and hole diameter (1.0 mm).

The orifice plate generates hydrodynamic cavitation by causing an abrupt pressure drop as the liquid passes through the 1.0 mm diameter holes. The subsequent collapse of bubbles in the pressure recovery zone produces intense turbulence, enhancing mass transfer during transesterification, consistent with findings reported in the literature [38,41].

2.2.3. Geometric Design Parameters of the Plate

The geometric configuration of the orifice plate was designed considering two geometric parameters commonly used in cavitation.

- α = 4.0 mm^{-1}, the ratio between the total perimeter of the holes and the total flow area, selected according to values reported in previous studies [44,46].

- β = 0.030, the ratio between the total area of the holes and the cross-sectional area of the pipe, consistent with values reported for HC devices [43].

The geometric parameters and technical specifications of the orifice plate are summarized in Table 2.

Table 2. Technical specifications and geometric design parameters of the orifice plate used in the cavitator reactor.

Parameter	Value
Tube diameter	25 mm
Orifice plate diameter	25 mm
Orifice diameter	1.0 mm
Number of orifices	19
Plate thickness	3 mm
Material	Stainless steel
Distribution	Radial pattern
Total orifice area	14.92 mm^2
Tube area	490.87 mm^2
Total orifice perimeter	59.66 mm
Parameter α	4.0 mm^{-1}
Parameter β	0.030

2.3. Experimental Design

A 3^2 factorial design was used with two quantitative factors (A and B), each evaluated at three levels, resulting in nine experimental combinations. This design, combined with the response surface methodology, allows for the simultaneous evaluation of the main effects of each factor and their interactions. Each combination was replicated twice, for a total of 18 experimental runs. The variation in biodiesel yield between replicate runs was always less than 1%, indicating excellent experimental reproducibility. The factors and their coded levels (−1 for low level, 0 for medium level, and +1 for high level) are shown in Table 3. Factor A corresponded to the feed pressure, evaluated at 1.72, 2.41, and 3.10 bar, measured upstream of the orifice plate. Factor B corresponded to the methanol:oil molar ratio, evaluated at 6:1, 8:1, and 10:1.

Table 3. Experimental factors and coded levels.

Code	Factor	Units	Levels		
			−1	**0**	**1**
A	Feed pressure	bar	1.72	2.41	3.1
B	Molar ratio	—	6:01	8:01	10:01

During all tests, the reaction time (45 min), NaOH concentration (1 wt% relative to the oil mass), reaction temperature (60 ± 5 °C), and cavitator reactor configuration, including the previously described orifice plate, were kept constant. Although reaction time is a relevant parameter in transesterification, in this work it was kept constant because the objective of the study was not to perform a kinetic analysis, but rather to evaluate the combined effect of hydrodynamic and stoichiometric variables on the performance of the process under stable and reproducible operating conditions.

Feed pressure and methanol:oil molar ratio were selected as the main independent variables due to their direct and complementary influence on process intensification. Previous studies have reported that feed pressure controls the pressure drop across the orifice plate and, therefore, the intensity of cavitation and mass transfer [50].

The molar ratio of methanol to oil influences the availability of the alcoholic reagent and shifts the equilibrium of the transesterification reaction, effects that are particularly relevant under conditions of intensified mixing due to HC [51]. The ranges evaluated were defined considering the operating criteria of the system and values widely reported in the literature [52,53].

The experimental design was generated using Design-Expert® software, version 12.

2.4. Experimental Procedure

The experimental procedure began with thermal conditioning of the system. Hot water supplied from a thermoregulated bath was circulated through the jacketed tank until a working temperature of 60 ± 5 °C was reached, monitored by an installed sensor. The cooling flow was then adjusted to maintain stable thermal conditions during the reaction.

Soybean oil was subsequently introduced into the tank, and the recirculation pump was activated to ensure uniform flow through the orifice plate-type HC reactor. After a 15 min stabilization period, a small initial fraction was discharged to remove residual water.

Simultaneously, sodium methoxide (CH_3ONa) was prepared by dissolving NaOH in methanol, which was added gradually to control heat release, in accordance with Aeamsuksai et al. [54]. The mixture was magnetically stirred for approximately 1 h until a clear, homogeneous solution was obtained. The catalyst concentration was 1 wt% relative to the oil. Each run used 3 L of oil (density 0.920 g/mL; 2760 g), corresponding to 27.6 g of NaOH dissolved in methanol according to the evaluated methanol:oil molar ratios (6:1, 8:1, and 10:1).

When the system reached operating temperature and the flow was stable, the working pressures (1.72, 2.41, and 3.10 bar) were adjusted using valves V1 and V2. Subsequently, the sodium methoxide solution was added gradually, initiating the HC-assisted transesterification reaction under conditions similar to those reported by Thakkar [34]. The reactive mixture circulated continuously through the stainless steel orifice plate reactor for 45 min.

Previous studies have shown that the orifice plate generates microbubbles that collapse and release localized energy, improving mixing and promoting emulsification between methanol and oil [46]. Furthermore, reports indicate that this phenomenon contributes to achieving high biodiesel yields in HC systems [42].

At the end of the reaction, recirculation was stopped to allow phase separation, yielding an upper biodiesel layer and a lower glycerol layer. The glycerol was discharged through valve V3 to avoid remixing, and the crude biodiesel was transferred to separatory funnels for purification. The biodiesel was washed with hot distilled water (60 °C) to remove residual catalyst, methanol, and soaps until the rinse water became clear, and subsequently dried at 60 °C for 24 h to eliminate residual moisture, obtaining a transparent, bright yellow product without turbidity.

2.5. Statistical Analysis

The experimental data were analyzed using analysis of variance (ANOVA) to determine the statistical significance of the factors and their interactions on biodiesel yield, with a confidence level of 95% ($p < 0.05$). A second-order polynomial model was used to predict the optimal response.

2.6. Characterization of Biodiesel

The purified biodiesel obtained under optimal conditions was characterized to assess its quality and verify compliance with international specifications ASTM D6751 [55] and EN 14214 [56]. The following standardized methods were applied: density at 15 °C (EN ISO 12185) [57], kinematic viscosity at 40 °C (ASTM D445) [58], acid value (ASTM D664) [59], sulfate ash (ASTM D874) [60], sulfur content (ASTM D5453) [61], moisture content (EN

ISO 12937, Karl Fischer method) [62], lower heating value (ASTM D240) [63], and carbon residue (ASTM D4530) [64].

2.7. Determination of Biodiesel Yield

The biodiesel yield percentage was calculated using Equation (1). This equation compares the mass of dry biodiesel obtained after purification with the initial mass of vegetable oil used in the reaction.

$$R(\%) = \frac{m_{biodiesel}}{m_{oil}} \cdot 100 \quad (1)$$

where R is the biodiesel yield percentage, $m_{biodiesel}$ is the mass of the dry biodiesel obtained after the purification process, and m_{oil} corresponds to the initial mass of oil used as the feedstock.

3. Results and Discussion

The results corresponding to the nine experimental conditions, each evaluated in duplicate (n = 2), are presented in Table 4. Biodiesel yields, expressed as mean ± standard deviation, ranged from 78.67 ± 0.11% to 92.98 ± 0.24%, along with acid value, soap formation, and density values. The low standard deviations observed within each treatment indicate good reproducibility of the experimental method.

Table 4. Average results of the biodiesel production process by hydrodynamic cavitation under different operating conditions (mean ± standard deviation, n = 2 replicates).

Test	Feed Pressure (bar)	Molar Ratio	Yield (%)	Acid Value (mg KOH/g)	Amount of Soap (ppm)	Density (g/mL)
1	1.72	6:1	84.58 ± 0.62	0.240 ± 0.000	307.279 ± 0.000	0.89881 ± 0.00063
2	1.72	8:1	87.02 ± 0.12	0.237 ± 0.006	408.275 ± 0.462	0.89608 ± 0.00494
3	1.72	10:1	78.67 ± 0.11	0.154 ± 0.005	244.255 ± 1.413	0.90042 ± 0.00042
4	2.41	6:1	84.63 ± 0.03	0.205 ± 0.007	328.895 ± 0.322	0.90037 ± 0.00024
5	2.41	8:1	90.77 ± 0.35	0.305 ± 0.007	298.941 ± 0.000	0.88608 ± 0.00520
6	2.41	10:1	82.20 ± 0.13	0.201 ± 0.001	342.500 ± 0.000	0.90044 ± 0.00027
7	3.10	6:1	88.24 ± 0.04	0.185 ± 0.000	325.326 ± 0.004	0.90024 ± 0.00014
8	3.10	8:1	92.98 ± 0.24	0.298 ± 0.011	305.267 ± 0.000	0.89103 ± 0.00213
9	3.10	10:1	83.00 ± 0.02	0.234 ± 0.002	370.526 ± 0.000	0.89978 ± 0.00123

Descriptive statistics for biodiesel yield among the different treatments are summarized in Table 5. The overall mean was 85.79% with a standard deviation of 4.45%, indicating considerable variability attributable to the effects of feed pressure and molar ratio on yield.

Table 5. Summary statistics of biodiesel yield across 9 experimental treatments.

Variable	N	Mean	Std. Dev.	Variance	Minimum	Median	Maximum
Yield	9	85.79	4.45	19.77	78.67	84.63	92.98

3.1. Statistical Analysis Using Response Surface Methodology

The response surface methodology (RSM) was applied to evaluate the main effects and interactions between the operating variables. Figure 5 shows the half-normal plot of effects, which allows for the visual identification of factors that significantly influence biodiesel yield.

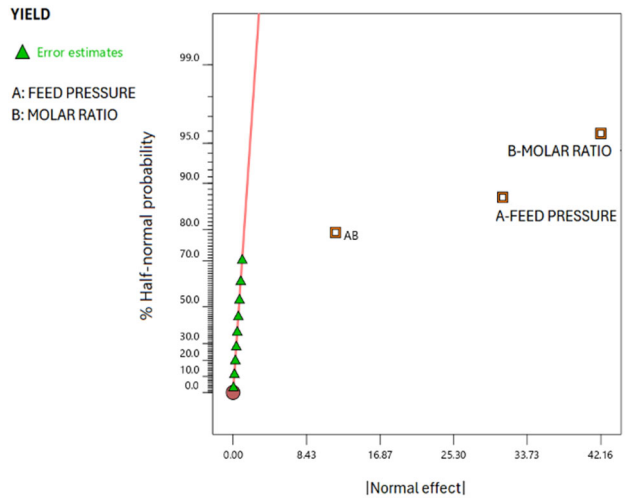

Figure 5. Half-normal plot of the effects of factors on biodiesel yield. Factors A (feed pressure) and B (methanol:oil molar ratio), as well as their interaction (AB), deviate from the reference line, indicating a significant influence ($p < 0.05$) on the response variable. The brown circle indicates a data point at the origin belonging to the group of non-significant effects.

The points that deviate from the red straight line represent statistically significant effects. It is clear that the feed pressure (A), the molar ratio (B), and the interaction between both factors (AB) are far from the line, confirming their significant influence on the response variable.

The analysis of variance (ANOVA) shown in Table 6 quantitatively confirms these effects. Both the feed pressure and the methanol:oil molar ratio, as well as their interaction, have statistically significant effects ($p < 0.0001$) on biodiesel yield.

Table 6. Analysis of variance (ANOVA) for biodiesel yield.

Source	Sum of Squares	Degrees of Freedom	Mean Square	F-Value	*p*-Value
Model	316.45	8	39.56	586.12	<0.0001 *
A—Feed pressure	64.97	2	32.49	481.34	<0.0001 *
B—Molar ratio	241.21	2	120.61	1787.05	<0.0001 *
Interactions (AB)	10.27	4	2.57	38.03	<0.0001 *
Pure error	0.6074	9	0.0675	—	—
Total sum of squares	317.06	17	—	—	—

Note: * $p < 0.0001$ (highly significant).

The response surface model exhibited an excellent fit ($R^2 = 0.9981$), indicating strong agreement between experimental and predicted values. The close agreement between adjusted R^2 (0.9964) and predicted R^2 (0.9923) confirms the robustness and predictive capability of the model. The low standard deviation (0.26) and coefficient of variation (0.30%) reflect high experimental precision. An adequate precision value of 77.93, well above the recommended minimum of 4, further validates the model within the evaluated design space.

A second-order polynomial model was developed to predict biodiesel yield using Equation (2), with variables coded at −1, 0, and +1.

$$R = 85.79 + 2.33A - 0.0397A^2 - 2.26B - 2.23B^2 + 0.1675AB - 0.525A^2B - 0.3283AB^2 + 0.1081A^2B^2 \quad (2)$$

where R is the biodiesel yield (%), A is the coded feed pressure (−1, 0, +1 for 1.72, 2.41, 3.10 bar), and B is the coded methanol:oil molar ratio (−1, 0, +1 for 6:1, 8:1, 10:1).

Although the second-order polynomial model includes higher-order interaction terms (A^2B, AB^2, and A^2B^2), these do not represent independent physical mechanisms but rather capture the nonlinear coupling of the system within the evaluated experimental domain. In HC-assisted transesterification, previous studies have shown that feed pressure controls cavitation intensity, droplet fragmentation, and interfacial area generation [33], while the methanol:oil molar ratio regulates the reaction equilibrium and the effectiveness of the interfacial catalyst [42].

Under these conditions, variations in pressure modify the effect of excess methanol in a non-linear manner, which is reflected mathematically in these terms. They are maintained to preserve the hierarchy of the model and its predictive capacity, while the physical interpretation of the process focuses mainly on the linear terms (A, B) and the primary interaction (AB). The linear terms (A and B) describe the direct effects of feed pressure and the methanol:oil molar ratio on biodiesel yield, while the quadratic terms (A^2 and B^2) represent the curvature associated with the intensification of cavitation and the limitations of the reaction equilibrium. The primary interaction (AB) reflects the synergistic effect between the two variables.

3.2. Statistical Validation of the Model

The validity of the model was evaluated through a comprehensive residual analysis, as shown in Figure 6.

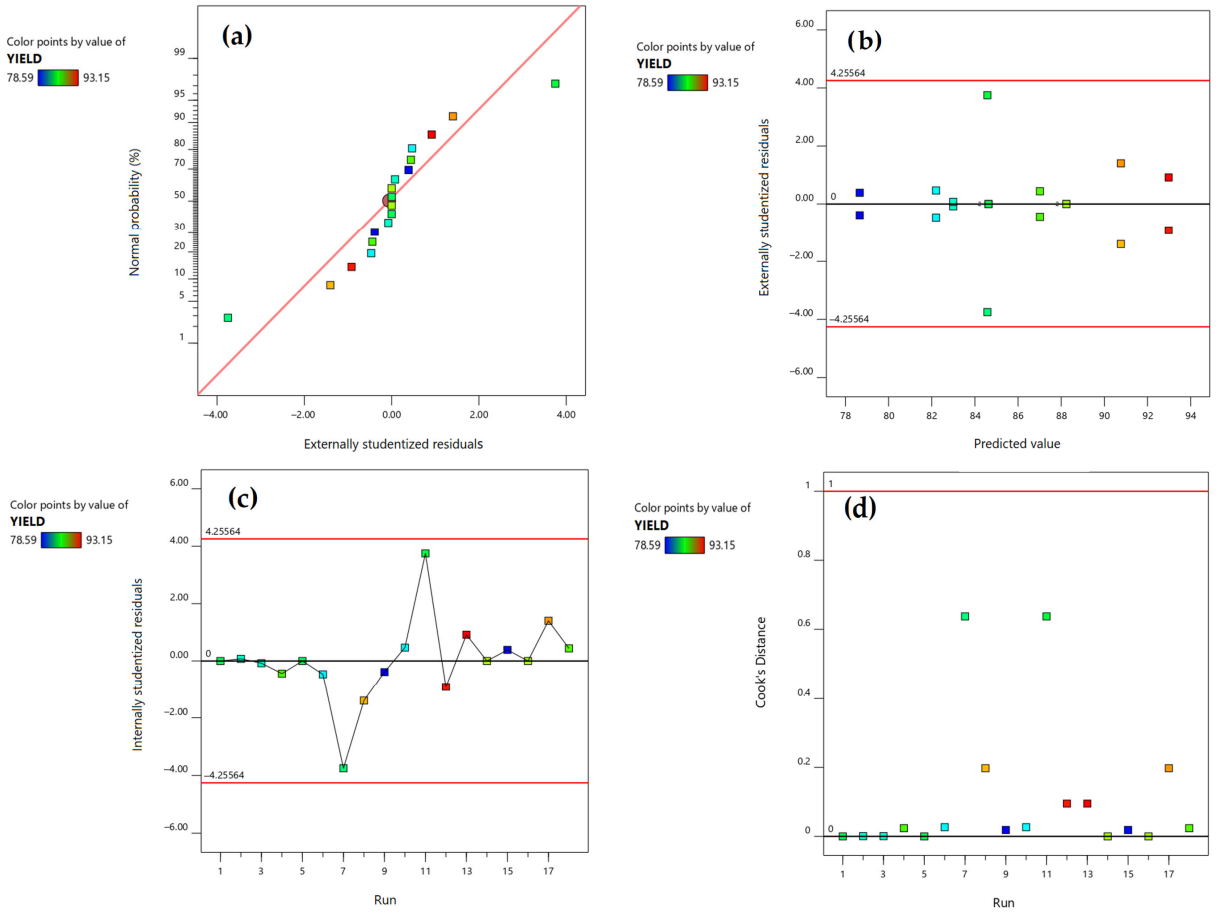

Figure 6. Diagnosis of the statistical model: (**a**) normal probability plot of residuals, confirming normal distribution; (**b**) residuals versus predicted values, showing random dispersion and constant variance; (**c**) residuals versus order of run, indicating independence; (**d**) Cook's distance, confirming absence of influential outliers.

As shown in Figure 6a, the normal probability plot indicates that the residuals align closely with the theoretical diagonal line, confirming that they follow a normal distribution. This condition is essential for the validity of the statistical inferences obtained through ANOVA.

Figure 6b presents the plot of residuals versus predicted values, which exhibits a random and uniform dispersion around zero, with no observable systematic patterns. This confirms homoscedasticity and the absence of outliers, validating the adequacy of the quadratic model without requiring any transformation of the response.

As shown in Figure 6c, the residuals plotted against the experimental run order display a random distribution, indicating that the sequence of experiments did not influence the results.

In Figure 6d, Cook's distance was used to evaluate the influence of each observation on the model coefficients. No data point exceeded the critical threshold of 1.0, confirming the absence of influential outliers.

The Box–Cox analysis was used to determine whether a transformation of the response variable is required, such as logarithmic, square root, or inverse transformations. The software recommended a transformation based on the estimated value of λ.

Although a value of $\lambda = -2.05$ was suggested, it was verified that $\lambda = 1$ lies within the 95% confidence interval. Therefore, no transformation was considered necessary, and the quadratic model was deemed adequate to describe the experimental data.

3.3. Effect of Feed Pressure

ANOVA revealed that feed pressure has a highly significant effect ($F = 481.34$, $p < 0.0001$) on biodiesel yield. The experimental results show a directly proportional relationship between pressure and yield. When the pressure increased from 1.72 to 2.41 bar, the average yield rose from 83.42% to 85.87%. At 3.10 bar, an average yield of 88.07% was obtained. This progressive increase of approximately 2.5 percentage points per 0.69 bar confirms that feed pressure is a determining factor in process efficiency.

The positive effect of pressure is attributed to the intensification of HC. According to previous studies [12], increasing the upstream pressure across the orifice plate generates a greater pressure drop, which enhances vapor cavity formation and promotes more energetic collapse events. The literature also reports that these collapses fragment oil droplets into smaller sizes, increasing the interfacial area between immiscible phases and thereby accelerating the transesterification reaction by improving contact between oil and methanol [65].

Although the cavitation number (σ) is a dimensionless parameter widely used to estimate the propensity to cavitate, it was not determined in this study because no local pressure and velocity measurements were taken in the cavitation region. To avoid introducing unverified assumptions, cavitation intensity was evaluated using measurable operating parameters, mainly feed pressure, used as an indirect indicator of the phenomenon. This approach has been previously used in studies with orifice plates when local measurements are not available, allowing for consistent analysis of the influence of cavitation on process performance [42,45].

3.4. Effect of the Methanol:Oil Molar Ratio

ANOVA indicated that the methanol:oil molar ratio was the most influential factor affecting biodiesel yield ($F = 1787.05$, $p < 0.0001$). The response exhibited nonlinear behavior with a clearly defined optimum. Experimental results showed that the 8:1 ratio produced the highest average biodiesel yield (90.26%), significantly higher than those obtained at 6:1 (85.82%) and 10:1 (81.29%). The difference of approximately nine percentage points between the optimum condition and the highest ratio suggests a critical balance in the amount of methanol supplied.

This optimum results from the balance between two opposing effects. Excess methanol shifts the equilibrium of the reversible transesterification reaction toward ester formation. At the same time, excessive methanol dilutes the effective concentration of the alkaline catalyst (1 wt% NaOH relative to the oil mass), reducing its catalytic efficiency. The 8:1 proportion corresponds to an excess of approximately 167% relative to the theoretical stoichiometric value (3:1), sufficient to drive the reaction forward without causing adverse effects. Beyond this point, further increases in methanol do not improve yield and may even negatively affect process performance.

In experiments conducted at a 10:1 ratio, longer settling times and a more diffuse glycerol–biodiesel interface were observed, indicating difficulties in phase separation. Previous studies [10] have reported that a significant fraction of glycerol and alcohol may remain in the ester phase, together with other impurities, thereby limiting the complete separation of crude biodiesel.

HC generates finer microemulsions and increases the interfacial area available for reaction, intensifying mass transfer and allowing higher conversion and biodiesel yield under the 8:1 condition compared with other methanol:oil ratios.

3.5. Analysis of the Interaction Between Variables

The ANOVA demonstrated a statistically significant interaction ($F = 38.03$, $p < 0.0001$) between feed pressure and methanol:oil molar ratio, indicating that the effect of one factor depends on the level of the other. Figure 7 presents a comparison between the experimental average yields obtained under each condition (bars) and the values predicted by the response surface model (dots).

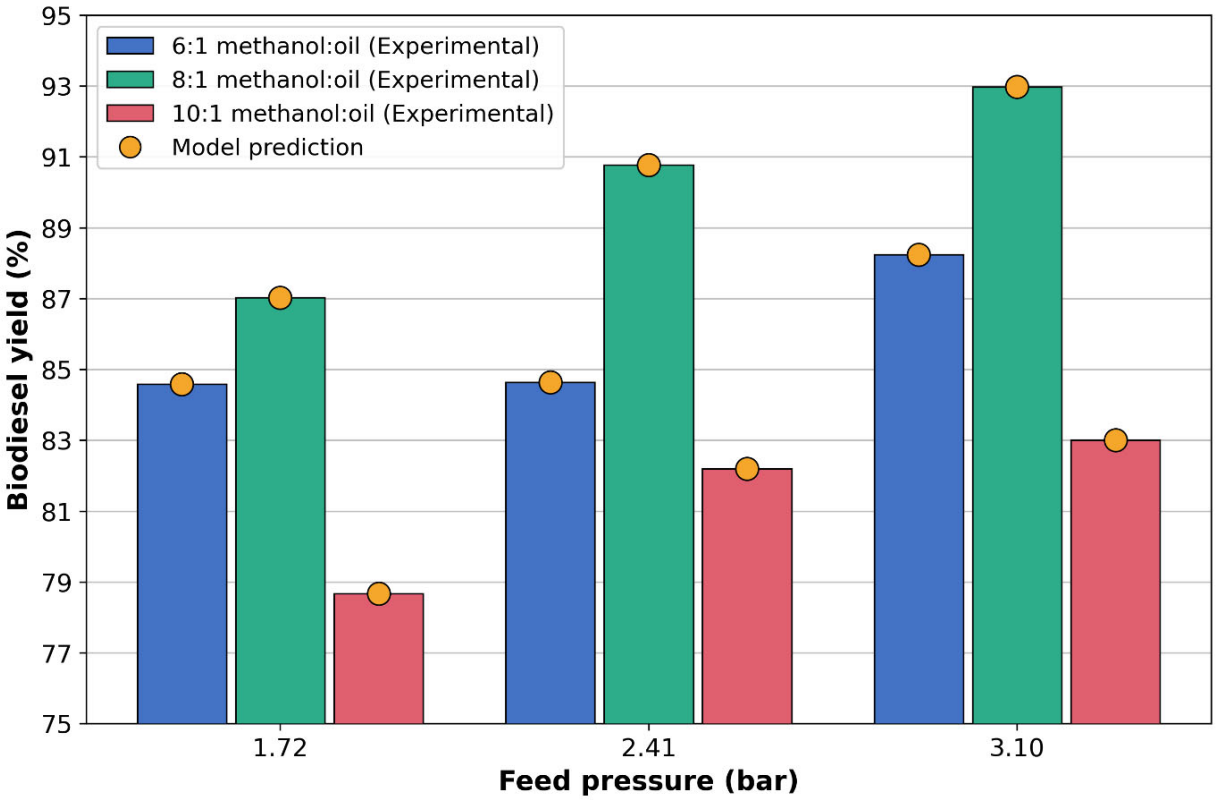

Figure 7. Biodiesel yield (%) as a function of feed pressure (bar) and methanol:oil molar ratio. Bars represent experimental mean values; dots represent model-predicted values.

At 1.72 bar, the model predicts an optimum yield at a molar ratio of 8:1 (87.02%), slightly higher than 6:1 (84.58%) and 10:1 (78.67%). Experimental averages in Table 4

confirm this behavior. However, the difference between 8:1 and 6:1 is only ~2.4 percentage points, suggesting that at low pressure the cavitation intensity is insufficient to fully capitalize on methanol excess.

At 2.41 bar, the interaction effect becomes more evident. The predicted yield at 8:1 increases to 90.77%, compared with 84.63% (6:1) and 82.20% (10:1). The experimental results closely follow this trend. The difference between 8:1 and 6:1 exceeds 6 percentage points, indicating that intermediate pressure enhances the effective utilization of excess methanol.

At 3.10 bar, the synergistic effect is maximized. Both model and experimental data show a yield of 92.98% at 8:1, significantly higher than 88.24% (6:1) and 83.00% (10:1). The gap between 8:1 and 10:1 approaches 10 percentage points, confirming that higher pressure intensifies cavitation and strengthens the interaction between pressure and molar ratio.

This interaction demonstrates that feed pressure not only increases biodiesel yield but also reinforces the superiority of the 8:1 molar ratio. At 1.72 bar, increasing the molar ratio from 6:1 to 8:1 improves yield by only 2.44 percentage points, indicating a marginal practical advantage under low cavitation intensity. In contrast, at 3.10 bar, the gap widens to 4.74 points, and the difference relative to 10:1 reaches 9.98 points, clearly establishing 8:1 as the optimal condition.

This behavior is attributed to intensified cavitation at higher pressures, which produces smaller droplets and enhances interfacial contact between oil and methanol. Under these conditions, the 8:1 ratio provides efficient reaction performance and high yield. Conversely, excessive methanol at 10:1 promotes catalyst dilution and hinders phase separation, consistent with experimental observations. In mechanically agitated systems, optimum molar ratios are typically close to 6:1, as the lower interfacial area limits the effective utilization of larger methanol excess.

Secondary properties of the crude biodiesel were also assessed. Density ranged from 0.886 to 0.900 g/mL (average 0.897 g/mL), with most values complying with ASTM D6751 specifications (0.860–0.900 g/mL). Density showed negligible dependence on operating conditions, indicating that it is primarily governed by the intrinsic composition of soybean oil. Soap content varied between 244 and 408 ppm. The optimal condition (3.10 bar, 8:1) yielded relatively low values (~305 ppm), whereas higher molar ratios (10:1) increased soap formation (342–371 ppm), suggesting that excess methanol favors secondary saponification reactions.

3.6. Physicochemical Characterization of Optimized Biodiesel

Biodiesel produced under optimal conditions (3.10 bar, molar ratio 8:1, 60 °C, 45 min, 1 wt% NaOH) was characterized using standard ASTM methods. Table 7 shows the results compared to the limits established in ASTM D6751 and EN 14214.

Table 7. Characterization of optimized biodiesel according to ASTM D6751 and EN 14214 specifications.

Test	Units	Results	Method	Limit
Density at 15 °C	g/mL	0.880	EN ISO 12185	0.86–0.90
Viscosity at 40 °C	mm^2/s	4.2	ASTM D445	1.9–6.0
Acid value	mg KOH/g	0.23	ASTM D664	≤0.50
Sulfated ash	wt%	0.002	ASTM D874	≤0.020
Sulfur content	wt%	0.03	ASTM D5453	≤0.050 (Grade S500)
Moisture content	wt%	0.092	EN ISO 12937	≤0.050
Lower heating value	MJ/kg	39.13	ASTM D240	—
Carbon residue	wt%	0.26	ASTM D4530	≤0.050

The biodiesel met ASTM D6751 Grade S500 requirements for key engine performance parameters, including kinematic viscosity (4.2 mm^2/s), acid value (0.23 mg KOH/g), sulfur

content (0.03%), and sulfate ash (0.002%). These values indicate efficient transesterification, low free fatty acid content, and minimal risk of corrosion or pollutant emissions. The measured density (0.880 g/mL) falls within the EN 14214 range (0.860–0.900 g/mL).

Although the biodiesel produced under optimal conditions satisfied most ASTM D6751 and EN 14214 criteria, moisture content (0.092 wt%) and carbon residue (0.26 wt%) exceeded the maximum permitted limit (0.05 wt%). These deviations are primarily attributed to post-reaction purification rather than to the HC-assisted transesterification process itself.

The high moisture content is associated with the use of aqueous washes employed to remove residual catalyst, soaps, and glycerol. It has been reported that biodiesel can retain water in the form of microemulsions stabilized by traces of methanol and surfactant compounds derived from saponification, which makes it difficult to completely remove by conventional thermal drying at atmospheric pressure [66]. Although drying at 60 °C for 24 h was applied in this study, this procedure may be insufficient to meet regulatory limits.

Similarly, high carbon residue is related to the presence of non-volatile impurities, such as residual glycerol, soaps, and partially converted triglyceride fractions, which tend to carbonize during the test. The use of high molar ratios of methanol, while favoring the shift in the reaction equilibrium, can hinder phase separation and promote the carryover of these compounds into the ester phase, increasing carbon residue [10].

In industrial applications, previous studies have shown that full compliance with ASTM and EN specifications is achieved through the integration of advanced purification and drying techniques, such as vacuum drying [67], dry purification with adsorbents or ion exchange resins [66], the use of molecular sieves [68], and natural bioadsorbents [69]. These strategies effectively reduce moisture content and carbon residue below regulatory limits, while also avoiding the generation of additional aqueous waste streams. Consequently, their incorporation would facilitate full compliance with fuel quality standards and reinforce the industrial viability of the proposed process.

Conventional aqueous washing was used in this study, a practice widely used at the laboratory scale due to its operational simplicity and experimental reproducibility. However, the future implementation of dry purification techniques could optimize the environmental performance and overall sustainability of the process.

Energy Considerations of the Process

Some previous studies suggest that hydrodynamic cavitation (HC) in biodiesel production could reduce the total energy demand of the process by approximately 40% compared to conventional mechanical agitation, due to improved mass transfer and shorter reaction times [41]. For conventional stirred reactors, energy is mainly used to maintain intense mixing for prolonged periods using high-power electric motors. In contrast, HC systems are reported to concentrate energy in localized areas of high intensity, which promotes the dispersion of methanol in the oil phase and accelerates the kinetics of transesterification [44].

In this study, intensification was achieved by passing the fluid through a cavitation reactor driven by a centrifugal pump, without using high-power agitation devices. Although energy consumption was not directly quantified, the pressures applied (1.72–3.10 bar) are moderate and compatible with standard centrifugal pumps, suggesting lower energy demand than conventional mechanical systems [10,25]. The literature indicates that hydrodynamic cavitation systems, due to enhanced microturbulence and increased interfacial area, can significantly improve energy efficiency and reduce reaction time compared to mechanical agitation [46]. However, a detailed quantitative analysis of energy consumption is considered a necessary step in future studies to accurately assess the specific efficiency of the process.

3.7. Comparison of Hydrodynamic Cavitation with Conventional and Alternative Methods

To evaluate the efficiency of HC, it was compared with the conventional mechanical stirring method (500 rpm, 60 ± 5 °C). The conventional method required 90 min to achieve 95% yield, while HC achieved 92.98% yield in 45 min under optimal conditions (3.10 bar, molar ratio 8:1, 60 ± 5 °C).

Additional experiments revealed that, after 20 min, HC achieved 92.90% yield compared to 20% for the conventional method, confirming the kinetic acceleration provided by HC, in agreement with previous reports [42].

Although the final yields are not identical, both methods achieved acceptable industrial levels (>90%), indicating that HC allows comparable yields to be achieved in substantially shorter reaction times than the conventional method.

Table 8 presents a systematic comparison of transesterification methods for the production of biodiesel from soybean oil, highlighting the advantages of HC in terms of reaction time, methanol:oil molar ratio, and operating conditions compared to technologies reported in the literature.

Table 8. Comparison of methods for producing biodiesel from soybean oil.

Transesterification Method	Catalyst (wt%)/Conditions	Temp. (°C)	Time (min)	Molar Ratio MeOH:Oil	Yield (%) [a,b]	Ref.
Hydrodynamic cavitation	NaOH, 1%	60 ± 5	45	8:1	93	This study
Conventional (mechanical stirring, homogeneous)	NaOH, 1%/ 500 rpm	60	90	6:1	95.0	This study
Conventional (mechanical stirring, homogeneous)	NaOH, 0.5%/ 700 rpm	60	120	12:1	98.58 [a]	[42]
Conventional (mechanical stirring, homogeneous)	KOH, 1%/ 700 rpm	60	120	9:1	97.1	[70]
Conventional (mechanical stirring, heterogeneous)	LiOH, 1.08%/ 500 rpm	65	72	8.9:1	98.8	[71]
Conventional (mechanical stirring, heterogeneous)	Li_2SiO_3, 10%/ 600 rpm	60	60	20:1	97.4	[72]
Conventional (mechanical stirring, heterogeneous)	Li_2TiO_3, 6%/ 300 rpm	65	120	24:1	98.5 [b]	[73]
Conventional (mechanical stirring, heterogeneous)	CaO, 7%	57.7	180	10:1	93.0	[74]
Microwave	SrFe/CaO (150 W)	60	56	10:1	98.87	[75]
Supercritical	Catalyst free (220 bar)	350	30	42:1	90.98	[76]
Supercritical	Catalyst free (180 bar)	300	150	42:1	80.11	[77]
Electrolysis	Catalyst free (22 V)	25	120	25:1	94.71	[78]

[a]: FAME content (%). [b]: Triglyceride (oil) conversion (%).

The data show that conventional homogeneous and heterogeneous methods, such as NaOH or Li-based catalysts, achieve slightly higher biodiesel performance, reaching yields of 98.8%, triglyceride conversion of 98.5%, or FAME content of 98.58%, but these methods require significantly longer reaction times and higher methanol:oil molar ratios. Alternative approaches for achieving high biodiesel yields, including microwave-assisted transesterification (98.87%), supercritical alcohol processing (90.98%), and electrolysis (94.71%), face similar limitations due to the need for excess methanol or extreme operating conditions. In contrast, HC achieves comparable results with a yield of 93% in a much shorter reaction time (45 min), at a moderate temperature (60 °C) and a lower methanol:oil ratio (8:1), highlighting its potential as an efficient process intensification technique for scalable biodiesel production.

3.8. Comparison of Performance with Previous Studies of Hydrodynamic Cavitation

In order to position the results obtained within the current context of HC applied to biodiesel production, a direct comparison was made with various studies reported in the literature. As shown in Table 9, the optimal conditions obtained in this study (3.10 bar,

methanol:oil molar ratio 8:1, 60 ± 5 °C, and 1 wt% NaOH) achieved a maximum yield of 93%, which allows for contextualization with previously reported HC configurations.

Table 9. Comparison of operating parameters and biodiesel performance in studies based on hydrodynamic cavitation.

Feedstock	HC Device Geometry	Pressure (bar)	Temp. (°C)	Molar Ratio MeOH:Oil	Catalyst (wt%)	Time (min)	Yield (%) [a,b]	Ref.
Soybean oil	19 holes, 1 mm Ø	3.10	60 ± 5	8:1	NaOH, 1%	45	93.0	This study
Soybean oil	7 holes, 2 mm Ø	7	62	4:1	KOH, 0.3%	30	98.0	[79]
Waste soybean oil	7 holes, 2 mm Ø	5.4	63 ± 1	4:1	KOH, 0.3%	40	98.0	[79]
Castor oil	7 holes, 3 mm Ø	4	60.3	9.82:1	KOH, 1.06%	50.8	92.27	[34]
Virgin soybean oil	21 holes, 1 mm Ø	2	60	5:1	CH_3ONa, 1%	15	97.0	[41]
Waste soybean oil	100 holes, 0.3 mm Ø	7	35 ± 2	6.8:1	NaOH, 1%	5	99.0	[43]
Hippophae rhamnoides oil	21 holes, 1 mm Ø	3	57.5 ± 2.5	6:1	KOH, 1%	15	96.5 [a]	[44]
Cannabis sativa L. oil	7 holes, 3 mm Ø	3	60	6:1	KOH, 1%	20	97.5	[45]
Microalgae extract	7 holes, 4 mm Ø	3.6	60	6.5:1	KOH, 1.301%	11.5	97.3	[52]
Thumba oil	20 holes, 2 mm Ø	2	80	6:1	TiO_2-Cu_2O, 1.6%	60	60.0 [b]	[80]
Thumba oil	3 holes, 2 mm Ø	2	60	6:1	TiO_2, 1.2%	60	71.8 [b]	[81]
Rendering pig fat	3 holes, 0.4 mm Ø	4.5	60	6:1	NaOH, 1%	10	87.54 [a]	[82]

[a]: FAME content (%). [b]: Triglyceride (oil) conversion (%). Ø: orifice diameter.

As shown in Table 9, HC systems reported in the literature typically operate at pressures of 2–7 bar and temperatures of 55–65 °C, achieving performance values between 87% and 99%, including biodiesel yield, FAME content, or triglyceride conversion, depending on the metric reported in each study. In this context, the value obtained in the present study (93%) falls within the expected range for HC reactors applied to vegetable oils.

Although some studies report values above 97%, a direct comparison must consider differences in feedstock type, device geometry, operating pressure, catalyst system, and the performance parameter evaluated, as these factors significantly influence the apparent efficiency of the process. The reactor evaluated in this study incorporates an alternative mechanical configuration and demonstrates competitive performance under operating conditions comparable to those reported in the specialized literature.

4. Conclusions

This study identified the optimal conditions for biodiesel synthesis via hydrodynamic cavitation-assisted transesterification of soybean oil: feed pressure of 3.10 bar, methanol:oil molar ratio of 8:1, temperature of 60 ± 5 °C, and 1 wt% NaOH catalyst. Under these conditions, a yield of 92.98% was achieved in 45 min. The conventional mechanical stirring method (60 °C, 500 rpm, 1 wt% NaOH) reached a yield of 95% after 90 min of reaction.

Key findings:

1. The HC reactor with a modular design using stainless steel universal joints allowed for quick assembly and disassembly of the orifice plate without interrupting the process circuit, representing an operational innovation compared to conventional designs that require complete disassembly with flanges and bolts. This configuration facilitated experimental operations and system maintenance at the laboratory scale, suggesting a potentially adaptable design for future scaling evaluations.
2. Feed pressure and methanol:oil molar ratio exhibited highly significant synergistic effects on biodiesel yield ($p < 0.0001$), accurately modeled by a second-order polynomial ($R^2 = 0.9981$).
3. The optimal ratio of 8:1, superior to the typical 6:1 ratio of conventional methods, demonstrates that cavitation improves interfacial contact, allowing efficient use of excess methanol without the phase separation difficulties observed at 10:1.

4. The biodiesel met ASTM D6751 specifications for kinematic viscosity, acid value, sulfur content, sulfate ash, and density, requiring further optimization for moisture and carbon residue.
5. Although HC showed high potential for intensification, optimizing the purification stage using water-free technologies is an area for improvement that would strengthen the sustainability of the proposed process.

Overall, the results show that HC is a viable technological alternative for the efficient production of biodiesel, evidenced by its ability to achieve high yields in reduced reaction times under the conditions evaluated, which supports its potential application in optimized biofuel processes.

Author Contributions: Conceptualization, J.T.M.-C.; methodology, J.T.M.-C., L.C.A.-M., J.A.-S. and E.W.V.-M.; software, L.C.A.-M. and J.A.-S.; validation, E.W.V.-M. and J.T.M.-C.; formal analysis, E.W.V.-M.; investigation, L.C.A.-M., J.A.-S., R.B.G.-S., L.O.-S.M. and F.A.T.-C.; resources, J.A.L.-H., J.A.M.-P. and S.A.V.-L.; data curation, L.C.A.-M., J.A.-S. and E.W.V.-M.; writing—original draft preparation, E.W.V.-M.; writing—review and editing, E.W.V.-M. and J.T.M.-C.; supervision, J.T.M.-C. and R.P.-S.; project administration, J.T.M.-C.; funding acquisition, J.A.L.-H., J.A.M.-P. and S.A.V.-L. All authors have read and agreed to the published version of the manuscript.

Funding: This research was funded by the Universidad Nacional del Callao, Lima, Perú.

Data Availability Statement: The original contributions of this study are included in the article. For further information, please contact the corresponding authors.

Acknowledgments: The authors thank the Universidad Nacional del Callao, Lima, Perú, especially the Vice-Rector of Research of the Universidad Nacional del Callao, for funding the publication of this article. The authors acknowledge the use of an artificial intelligence tool to support manuscript writing. All content was reviewed, verified, and validated by the authors, who take full responsibility for the content of this publication.

Conflicts of Interest: The authors declare no conflicts of interest.

References

1. United Nations. Transforming Our World: The 2030 Agenda for Sustainable Development. Available online: https://undocs.org/en/A/RES/70/1 (accessed on 27 October 2025).
2. IEA. Global Energy Review 2025. Available online: https://iea.blob.core.windows.net/assets/5b169aa1-bc88-4c96-b828-aaa50406ba80/GlobalEnergyReview2025.pdf (accessed on 28 October 2025).
3. United Nations Environment Programme. *Emissions Gap Report 2024: No More Hot Air . . . Please!* UNEP: Nairobi, Kenya, 2024. Available online: https://www.unep.org/resources/emissions-gap-report-2024 (accessed on 28 October 2025).
4. United Nations Framework Convention on Climate Change (UNFCCC). Paris Agreement. 2015. Available online: https://unfccc.int/sites/default/files/english_paris_agreement.pdf (accessed on 28 October 2025).
5. International Energy Agency (IEA). Global Biofuel Demand, Historical, Main and Accelerated Case, 2016–2028. Available online: https://www.iea.org/data-and-statistics/charts/global-biofuel-demand-historical-main-and-accelerated-case-2016-2028 (accessed on 29 October 2025).
6. Pydimalla, M.; Husaini, S.; Kadire, A.; Verma, R.K. Sustainable biodiesel: A comprehensive review on feedstock, production methods, applications, challenges and opportunities. *Mater. Today Proc.* **2023**, *92*, 458–464. [CrossRef]
7. Xu, H.; Ou, L.; Li, Y.; Hawkins, T.R.; Wang, M. Life cycle greenhouse gas emissions of biodiesel and renewable diesel production in the United States. *Environ. Sci. Technol.* **2022**, *56*, 7512–7521. [CrossRef]
8. Elgharbawy, A.S.; Farghali, M.; Osman, A.I.; Hanafy, M.A.; Al-Muhtaseb, A.H. Innovative biodiesel production for sustainable energy: Advances in feedstocks, transesterification, and cost efficiency. *Biomass Bioenergy* **2025**, *201*, 108114. [CrossRef]
9. Yu, G.W.; Nie, J.; Lu, L.G.; Wang, S.P.; Li, Z.G.; Lee, M.R. Transesterification of soybean oil by using the synergistic microwave-ultrasonic irradiation. *Ultrason. Sonochem.* **2017**, *39*, 281–290. [CrossRef] [PubMed]
10. Wan Osman, W.N.A.; Rosli, M.H.; Mazli, W.N.A.; Samsuri, S. Comparative review of biodiesel production and purification. *Carbon Capture Sci. Technol.* **2024**, *13*, 100264. [CrossRef]

11. Mhetras, N.; Gokhale, D. Sustainable biodiesel production: Importance of feedstock resources and production methods. *RSC Adv.* **2025**, *15*, 26739–26754. [CrossRef]
12. Patil, S.; Baral, S.; Dhanke, P. Hydrodynamic cavitation for process intensification of biodiesel synthesis—A review. *Curr. Res. Green Sustain. Chem.* **2021**, *4*, 100144. [CrossRef]
13. Masjudin; Chang, W.-C. Comparative study on saturated and unsaturated fatty acid methyl esters (FAME) composition in biodiesel production from waste soybean, sunflower, and canola oils. *Biofuels* **2025**, *17*, 1–24. [CrossRef]
14. Chen, R.; Xue, B.; Zhu, F.; Qiu, Y.; Wang, H.; Wang, Y.; Feng, H.; Wang, Y.; Zhou, T. The application of heterogeneous catalysts in esterification/ transesterification for biodiesel production. *Renew. Sustain. Energy Rev.* **2026**, *226*, 116262. [CrossRef]
15. Andreo-Martínez, P.; Ortiz-Martínez, V.M.; García-Martínez, N.; de los Ríos, A.P.; Hernández-Fernández, F.J.; Quesada-Medina, J. Production of biodiesel under supercritical conditions: State of the art and bibliometric analysis. *Appl. Energy* **2020**, *264*, 114753. [CrossRef]
16. Derobertis, F.; Leone, M.S.; Mesto, E.; Schingaro, E.; Porfido, C.; Ditaranto, N.; Mali, M.; Dell'Anna, M.M.; Mastrorilli, P. Microwave-assisted biodiesel production from waste cooking oil using steel slags as catalyst. *Eur. J. Inorg. Chem.* **2024**, *27*, e202400375. [CrossRef]
17. Razzak, S.A.; Zakir Hossain, S.M.; Ahmed, U.; Hossain, M.M. Cleaner biodiesel production from waste oils (cooking/vegetable/frying): Advances in catalytic strategies. *Fuel* **2025**, *393*, 134901. [CrossRef]
18. Demir, E.; Çalhan, S.D.; Sönmez, Ö. Microwave-assisted biodiesel production from waste cooking oil using deep eutectic solvent catalyst: Kinetic and thermodynamic insights. *Biomass Bioenergy* **2025**, *201*, 108148. [CrossRef]
19. Alabi, O.O.; Gbadeyan, O.J.; Bala, A.; Ogunsiji, G.O.; Deenadayalu, N. Study of combustion characteristics of diesel–vegetable oil blends utilizing an industrial fuel burner. *Fuel Commun.* **2024**, *18*, 100104. [CrossRef]
20. Zheng, F.; Cho, H.M. Study on biodiesel production: Feedstock evolution, catalyst selection, and influencing factors analysis. *Energies* **2025**, *18*, 2533. [CrossRef]
21. Jayakumar, M.; Karmegam, N.; Gundupalli, M.P.; Gebeyehu, K.B.; Asfaw, B.T.; Chang, S.W.; Ravindran, B.; Awasthi, M.K. Heterogeneous base catalysts: Synthesis and application for biodiesel production—A review. *Bioresour. Technol.* **2021**, *331*, 125054. [CrossRef]
22. Alemu, T.; Alemu, A.G. Recent developments in catalysts for biodiesel production applications. In *Advanced Biodiesel—Technological Advances, Challenges, and Sustainability Considerations*; IntechOpen: London, UK, 2023. [CrossRef]
23. Suhel, A.; Abdul Rahim, N.; Abdul Rahman, M.R.; Bin Ahmad, K.A. Biodiesel synthesis from waste animal fat using waste chicken eggshells derived heterogeneous catalysts: An optimization study through Taguchi model. *Results Eng.* **2025**, *28*, 107261. [CrossRef]
24. Naseef, H.H.; Tulaimat, R.H. Transesterification and esterification for biodiesel production: A comprehensive review of catalysts and palm oil feedstocks. *Energy Convers. Manag. X* **2025**, *26*, 100931. [CrossRef]
25. Sun, X.; Liu, S.; Manickam, S.; Tao, Y.; Yoon, J.Y.; Xuan, X. Intensification of biodiesel production by hydrodynamic cavitation: A critical review. *Renew. Sustain. Energy Rev.* **2023**, *179*, 113277. [CrossRef]
26. Zhang, M.; Jiao, X.; Ren, D.; Huang, C.; Li, Y.; Chen, D.; Huo, Z. Design of anti-saponification Ca-based catalyst with porous-shell structure from crustacean waste for biodiesel production. *Fuel* **2024**, *363*, 131006. [CrossRef]
27. Oyekunle, D.T.; Barasa, M.; Gendy, E.A.; Tiong, S.K. Heterogeneous catalytic transesterification for biodiesel production: Feedstock properties, catalysts and process parameters. *Process Saf. Environ. Prot.* **2023**, *177*, 844–867. [CrossRef]
28. Khan, M.A.; Sheikh, N.A.; Jadoon, K.Z.; Ayub, A.; Awotwe, T.W.; Tariq, R. Utilization of locally sourced waste fats for biodiesel production: Experimental characterization and environmental life cycle assessment. *Biomass Bioenergy* **2025**, *194*, 107692. [CrossRef]
29. Alahmar, N.M.; Azelee, N.I.B.W.; Toemen, S. Efficient biodiesel production from waste cooking oil using a bifunctional Ce/Mn/γ-Al_2O_3 catalysts. *Sci. Rep.* **2025**, *15*, 352. [CrossRef]
30. Ceran, Z.D.; Demir, V.; Akgün, M. Optimization and kinetic study of biodiesel production from *Jatropha curcas* oil in supercritical methanol environment using ZnO/γ-Al_2O_3 catalyst. *Biomass Convers. Biorefin.* **2025**, *15*, 3903–3914. [CrossRef]
31. El Nagy, H.A.; Mohamed, M.A.E.A. Stable diesel microemulsion using diammonium ionic liquids and their effects on fuel properties, particle size characteristics and combustion calculations. *Sci. Rep.* **2024**, *14*, 7728. [CrossRef]
32. Mohod, A.V.; Subudhi, A.S.; Gogate, P.R. Intensification of esterification of non edible oil as sustainable feedstock using cavitational reactors. *Ultrason. Sonochem.* **2017**, *36*, 309–318. [CrossRef] [PubMed]
33. Zheng, H.; Zheng, Y.; Zhu, J. Recent developments in hydrodynamic cavitation reactors: Cavitation mechanism, reactor design, and applications. *Engineering* **2022**, *19*, 180–198. [CrossRef]
34. Thakkar, K.; Kachhwaha, S.S.; Kodgire, P. Multi-response optimization of transesterification reaction for biodiesel production from castor oil assisted by hydrodynamic cavitation. *Fuel* **2022**, *308*, 121907. [CrossRef]
35. Xia, G.; Manickam, S.; Yoon, J.Y.; Boczkaj, G.; Wang, W.; Wang, B.; Sun, X. Technological advances and applications of rotational hydrodynamic cavitation reactors for process intensification: A comprehensive review. *Chem. Eng. J.* **2025**, *522*, 167152. [CrossRef]

36. Zhang, X.; Lin, R.; Zhang, L.; Chen, J.; Li, M.; Wang, Y. Numerical investigation of effect of geometric parameters on performance of rotational hydrodynamic cavitation reactor. *Ultrason. Sonochem.* **2024**, *103*, 106790. [CrossRef]
37. Chaudhuri, J.H.; Chatterjee, D. Modelling of chemical kinetics in the presence of hydrodynamic cavitation for wastewater treatment applications. *Chem. Eng. Sci.* **2024**, *295*, 120167. [CrossRef]
38. Lei, E.; Yuan, X.; Xiang, K.; Shao, Z.; Hong, F.; Huang, Y. Research progress of hydrodynamic cavitation reactors in the field of water treatment: A review. *J. Water Process Eng.* **2024**, *66*, 105997. [CrossRef]
39. Khater, M.; Aboelazayem, O.; Ismail, A.R.; Soliman, A.; Amr, S.A.A.; El-Gendy, N.S.; Ezzat, A.A. Rotor–stator hydrodynamic cavitation reactor for intensification of castor oil biodiesel production. *Int. J. Environ. Sci. Technol.* **2025**, *22*, 4847–4868. [CrossRef]
40. Vera-Rozo, J.R.; Caicedo-Peñaranda, E.A.; Riesco-Ávila, J.M. Hydrodynamic cavitation in shockwave-power-reactor-assisted biodiesel production in continuous from soybean and waste cooking oil. *Energies* **2025**, *18*, 2761. [CrossRef]
41. Innocenzi, V.; Prisciandaro, M. Technical feasibility of biodiesel production from virgin oil and waste cooking oil: Comparison between traditional and innovative process based on hydrodynamic cavitation. *Waste Manag.* **2021**, *122*, 15–25. [CrossRef]
42. Vera-Rozo, J.R.; Riesco-Ávila, J.M.; Poveda-Pachon, M.Y.; Zaleta-Aguilar, A. Biodiesel production by hydrodynamic cavitation through an orifice plate. *Chem. Eng. Trans.* **2022**, *92*, 565–570. [CrossRef]
43. Bargole, S.; George, S.; Saharan, V.K. Improved rate of transesterification reaction in biodiesel synthesis using hydrodynamic cavitating devices of high throat perimeter to flow area ratios. *Chem. Eng. Process. Process Intensif.* **2019**, *139*, 1–13. [CrossRef]
44. Alsaiari, M.; Bokhari, A.; Chuah, L.F.; Mubashir, M.; Harraz, F.A.; Almohana, A.I.; Show, P.L.; Awasthi, M.K.; Rizk, M.A. Synthesis of methyl esters from *Hippophae rhamnoides* via pilot scale hydrodynamic cavitation intensification reactor. *Renew. Energy* **2023**, *205*, 238–247. [CrossRef]
45. Khan, I.A.; Prasad, N.; Pal, A.; Yadav, A.K. Efficient production of biodiesel from *Cannabis sativa* oil using intensified transesterification (hydrodynamic cavitation) method. *Energy Sources Part A Recover. Util. Environ. Eff.* **2020**, *42*, 2461–2470. [CrossRef]
46. Bokhari, A.; Chuah, L.F.; Yusup, S.; Klemeš, J.J.; Akbar, M.M.; Kamil, R.N.M. Cleaner production of rubber seed oil methyl ester using hydrodynamic cavitation: Optimisation and parametric study. *J. Clean. Prod.* **2016**, *136*, 31–41. [CrossRef]
47. Chuah, L.F.; Osman, N.H.; Kafi, A.; Mokhtar, K.; Bakar, A.A.; Zainuddin, N.; Abdullah, M.A.; Maruf, M.; Mahmud, S.M.; Loke, K.B. A review of intensification technology hydrodynamic cavitation in biodiesel production. *Chem. Eng. Trans.* **2024**, *114*, 637–642. [CrossRef]
48. Roy, S.; Rudra, S.; Muhandiram, D.I.; Roshid, M.M. Numerical modelling and experimental validation of an orifice plate-based hydrodynamic cavitation process for improving biomass pretreatment. *Biotechnol. Rep.* **2025**, *48*, e00925. [CrossRef] [PubMed]
49. Bimestre, T.A.; Júnior, J.A.M.; Canettieri, E.V.; Tuna, C.E. Hydrodynamic cavitation for lignocellulosic biomass pretreatment: A review of recent developments and future perspectives. *Bioresour. Bioprocess.* **2022**, *9*, 7. [CrossRef]
50. Zhou, P.; Zhong, K.; Zhu, Y. Numerical study of hydrodynamic cavitation pretreatment of food waste: Effect of pressure drop on the cavitation behavior. *Processes* **2024**, *12*, 300. [CrossRef]
51. Contreras, D.J.; Gomez, L.A.; Malagón-Romero, D. Evaluation of biodiesel production in a hydrodynamic cavitation reactor from waste cooking oil. *Chem. Eng. Trans.* **2022**, *91*, 601–606. [CrossRef]
52. Khan, T.A.; Khan, T.A.; Yadav, A.K. A hydrodynamic cavitation-assisted system for optimization of biodiesel production from green microalgae oil using a genetic algorithm and response surface methodology approach. *Environ. Sci. Pollut. Res.* **2022**, *29*, 49465–49477. [CrossRef] [PubMed]
53. Bizualem, Y.D.; Nurie, A.G. A review on recent biodiesel intensification process through cavitation and microwave reactors: Yield, energy, and economic analysis. *Heliyon* **2024**, *10*, e24643. [CrossRef] [PubMed]
54. Aeamsuksai, N.; Mueansichai, T.; Charoensuppanimit, P.; Kim-Lohsoontorn, P.; Aiouache, F.; Assabumrungrat, S. Comparison of different synthesis schemes for production of sodium methoxide from methanol and sodium hydroxide. *Eng. J.* **2020**, *24*, 63–77. [CrossRef]
55. *ASTM D6751-24*; Standard Specification for Biodiesel Fuel Blendstock (B100) for Middle Distillate Fuels. ASTM International: West Conshohocken, PA, USA, 2024.
56. *EN 14214:2012+A2:2019*; Liquid Petroleum Products—Fatty Acid Methyl Esters (FAME) for Use in Diesel Engines and Heating Applications—Requirements and Test Methods. CEN: Brussels, Belgium, 2019.
57. *EN ISO 12185:2024*; Crude Petroleum, Petroleum Products and Related Products—Determination of Density—Laboratory Density Meter with an Oscillating U-tube Sensor. ISO: Geneva, Switzerland, 2024.
58. *ASTM D445-24*; Standard Test Method for Kinematic Viscosity of Transparent and Opaque Liquids (and Calculation of Dynamic Viscosity). ASTM International: West Conshohocken, PA, USA, 2024.
59. *ASTM D664-24*; Standard Test Method for Acid Number of Petroleum Products by Potentiometric Titration. ASTM International: West Conshohocken, PA, USA, 2024.
60. *ASTM D874-23*; Standard Test Method for Sulfated Ash from Lubricating Oils and Additives. ASTM International: West Conshohocken, PA, USA, 2023.

61. *ASTM D5453-25*; Standard Test Method for Determination of Total Sulfur in Light Hydrocarbons, Spark Ignition Engine Fuel, Diesel Engine Fuel, and Engine Oil by Ultraviolet Fluorescence. ASTM International: West Conshohocken, PA, USA, 2025.
62. *EN ISO 12937:2000*; Petroleum Products—Determination of Water—Coulometric Karl Fischer Titration Method. ISO: Geneva, Switzerland, 2000.
63. *ASTM D240-25*; Standard Test Method for Heat of Combustion of Liquid Hydrocarbon Fuels by Bomb Calorimeter. ASTM International: West Conshohocken, PA, USA, 2025.
64. *ASTM D4530-25*; Standard Test Method for Determination of Carbon Residue (Micro Method). ASTM International: West Conshohocken, PA, USA, 2025.
65. Carpenter, J.; Pinjari, D.V.; Saharan, V.K.; Pandit, A.B. Critical review on hydrodynamic cavitation as an intensifying homogenizing technique for oil-in-water emulsification: Theoretical insight, current status, and future perspectives. *Ind. Eng. Chem. Res.* **2022**, *61*, 10587–10602. [CrossRef]
66. Jariah, N.F.; Hassan, M.A.; Hin Taufiq-Yap, Y.; Roslan, A.M. Technological advancement for efficiency enhancement of biodiesel and residual glycerol refining: A mini review. *Processes* **2021**, *9*, 1198. [CrossRef]
67. Tambun, R.; Burmana, D.A.; Haryanto, B.; Alexander, V. The Effect of vacuum process on biodiesel production from palm kernel fatty acid distillate. *Chem. Ind. Chem. Eng. Q.* **2024**, *30*, 73–79. [CrossRef]
68. Lin, C.Y.; Ma, L. Comparison of water-removal efficiency of molecular sieves vibrating by rotary shaking and electromagnetic stirring from feedstock oil for biofuel production. *Fermentation* **2021**, *7*, 132. [CrossRef]
69. Arenas, E.; Villafán-Cáceres, S.M.; Rodríguez-Mejía, Y.; García-Loyola, J.A.; Masera, O.; Sandoval, G. Biodiesel dry purification using unconventional bioadsorbents. *Processes* **2021**, *9*, 194. [CrossRef]
70. Encinar, J.M.; González, J.F.; Martínez, G.; Nogales-Delgado, S. Transesterification of soybean oil through different homogeneous catalysts: Kinetic study. *Catalysts* **2022**, *12*, 146. [CrossRef]
71. Mora, M.R.; Lacson, C.F.Z.; Choi, A.E.S.; Chung, T.-W.; Retumban, J.D.; Abarca, R.R.M.; Grisdanurak, N.; de Luna, M.D.G. Biodiesel production from soybean oil via LiOH-pumice catalytic transesterification and BBD-RSM optimization. *Energy Rep.* **2024**, *11*, 4032–4043. [CrossRef]
72. Chen, Y.-C.; Lin, D.-Y.; Chen, B.-H. Metasilicate-based catalyst prepared from natural diatomaceous earth for biodiesel production. *Renew. Energy* **2019**, *138*, 1042–1050. [CrossRef]
73. Dai, Y.M.; Kao, I.H.; Chen, C.C. Evaluating the optimum operating parameters of biodiesel production process from soybean oil using the Li_2TiO_3 catalyst. *J. Taiwan Inst. Chem. Eng.* **2017**, *70*, 260–266. [CrossRef]
74. Goli, J.; Sahu, O. Development of heterogeneous alkali catalyst from waste chicken eggshell for biodiesel production. *Renew. Energy* **2018**, *128*, 142–154. [CrossRef]
75. Chavez-Esquivel, G.; Ortega-Hernández, J.M.; García-Camacho, G.G.; García-Martínez, J.C.; Tavizón-Pozos, J.A. Microwave-assisted transesterification of soybean oil using eggshell-derived SrFe/CaO catalysts. *BioEnergy Res.* **2025**, *18*, 82. [CrossRef]
76. Qiao, B.Q.; Zhou, D.; Li, G.; Yin, J.Z.; Xue, S.; Liu, J. Process enhancement of supercritical methanol biodiesel production by packing beds. *Bioresour. Technol.* **2017**, *228*, 298–304. [CrossRef] [PubMed]
77. Zhou, D.; Qi, L.; Qiao, B.Q.; Xu, Q.Q.; Yin, J.Z. Continuous production of biodiesel from soybean flakes by extraction coupling with transesterification under supercritical conditions. *J. Supercrit. Fluids* **2017**, *120*, 395–402. [CrossRef]
78. Nguyen, H.C.; Aregawi, B.H.; Fu, C.-C.; Ong, H.C.; Barrow, C.J.; Su, C.-H.; Wu, S.-J.; Juan, H.-Y.; Wang, F.-M. Biodiesel production through electrolysis in the presence of choline chloride-based deep eutectic solvent: Optimization by response surface methodology. *J. Mol. Liq.* **2023**, *379*, 121633. [CrossRef]
79. Jeur, S.T.; Sorate, K.A.; Bhale, P.V. Energy-efficient biodiesel production via hydrodynamic cavitation: Comparative study of soybean and waste cooking oil. *Energy Convers. Manag.* **2026**, *348*, 120577. [CrossRef]
80. Patil, A.; Baral, S.S.; Dhanke, P.; Kore, V. Biodiesel production using prepared novel surface functionalised TiO_2 nano-catalyst in hydrodynamic cavitation reactor. *Mater. Today Proc.* **2020**, *27*, 198–203. [CrossRef]
81. Patil, A.D.; Baral, S.S. Process intensification of thumba methyl ester (biodiesel) production using hydrodynamic cavitation. *Chem. Eng. Res. Des.* **2021**, *171*, 277–292. [CrossRef]
82. Díez, D.; Urueña, A.; Barrios, C.; Antolín, G. Valorization of rendering fats to produce biodiesel by single and multi-orifice plate cavitation reactor. *Waste Biomass Valor.* **2019**, *10*, 3773–3780. [CrossRef]